Compression and rebound characteristics of agricultural sandy pasture soils from South Greenland

Pesch, Charles; Lamandé, Mathieu; de Jonge, Lis Wollesen; Norgaard, Trine; Greve, Mogens Humlekrog; Moldrup, Per

Published in:
Geoderma

DOI (link to publication from Publisher):
10.1016/j.geoderma.2020.114608

Publication date:
2020

Document Version
Accepted author manuscript, peer reviewed version

Compression and rebound characteristics of agricultural sandy pasture soils from South Greenland

Charles Pesch[a,*], Mathieu Lamandé[b,c], Lis Wollesen de Jonge[b], Trine Norgaard[b], Mogens Humlekrog Greve[b], Per Moldrup[a]

[a] *Aalborg University, Department of the Built Environment (BUILD), Thomas Manns Vej 23, DK-9220 Aalborg, Denmark*

[b] *Aarhus University, Department of Agroecology, Research Center Foulum, Blichers Allé 20, P.O. Box 50, DK-8830 Tjele, Denmark*

[c] *Norwegian University of Life Sciences, Faculty of Environmental Sciences and Natural Resource Management, Campus Ås, Universitetstunet 3, 1430 Ås, Norway*

Abstract

The reduction of permafrost areas and a prolonged vegetation period, both due to the ongoing climate change, open up new possibilities for agricultural activities in the circumpolar region. Presently, not much is known about the physical and functional properties of subarctic agricultural soils, making it challenging to evaluate soil impacts from increased agricultural activity. This study aims at assessing the mechanical properties of sandy Greenlandic pasture soils regarding a potential future land-use change.

The compression curves of 210 undisturbed soil core samples of three pasture fields in South Greenland and, as comparison, four intensively cultivated agricultural fields in Denmark were generated by uniaxial confined compression tests (UCCT). Four soil mechanical properties were determined: the precompression stress (σ_{pc}) as a measure of soil strength, the compression index (C_c) as a measure of compressibility, the swelling index (C_s) as a measure of resilience to compaction and the rebound ($\Delta\varepsilon$) after a relaxation time of 60 seconds as a measure of short-time recovery from compaction.

The Greenlandic pasture soils exhibited significantly higher σ_{pc} than the Danish cultivated soils despite their significantly lower initial bulk density, ρ_b. The C_c negatively correlated with ρ_b, and the Greenlandic soils showed higher C_c values than the Danish soils. The C_s showed a reciprocal correlation with ρ_b and, partly due to lower ρ_b of the Greenlandic soils, higher C_s than the Danish soils. The South Greenlandic sandy pasture soils showed compression and rebound characteristics on level with Danish loamy cultivated soils, likely due to a high content of particulate organic matter (non-degraded organic matter, including grass root-mat residues).

Keywords: Arctic pasture soils, Temperate cultivated soils, Precompression stress, Compression index, Swelling index, Rebound

1. Introduction

The ongoing climate change in the northern circumpolar region has consequences for the native population. The reduction of permafrost areas and an extending vegetation period, due to rising temperatures (Park et al., 2016) along with advances in plant breeding, can be useful for self-support in agricultural goods (Reykdal et al., 2016). Healthy soil is the primary element to allow and maintain a sustainable and productive agriculture. The effects of intensifying agricultural production, for example, of cattle grazing on the young and rather undeveloped Greenlandic soils, showed increased soil erosion (Jacobsen, 1987; Austrheim et al., 2008). The land-use intensification eventually will lead to an increase of fodder production and, thus, to higher and more frequent mechanical loads applied during traffic and tillage in the fields.

*Corresponding author
Email address: cp@civil.aau.dk (Charles Pesch)

Accepted: 16 July 2020; Available online: 18 August 2020 *Geoderma*

Existing literature suggests that agricultural traffic is a major source of detrimental soil compaction (Håkansson et al., 1988; Schjønning et al., 2015). Additionally, the change from perennial grassland to arable land will make soil tillage more frequent and may contribute to degrading changes in the soil's physical and functional properties by disturbing the present soil-ecological equilibrium.

Soil compaction negatively affects most of the soil physical (Horn, 2003), chemical (Lipiec and Stepniewski, 1995) and biological (Whalley et al., 1995; Beylich et al., 2010) properties, what almost unexceptionally leads to a decrease in yield (Alakukku and Elonen, 1995). Other studies on similar soils investigating the effect of grazing and trampling on pasture soils in circumpolar regions (Peth and Horn, 2006), attributed the negative impact of agricultural use on those lands not primarily to the compaction caused by trampling, but more to the change of soil cover, respectively a shift in cover-constituting plant communities due to grazing and a resulting change in the thermal and water-retention properties.

Only a few studies have investigated soil mechanical properties of arable land transformed to permanent pasture. Ajayi and Horn (2016) found a significant increase in mechanical soil resilience as well as an increase in pore rigidity. The opposite process, changing permanent grassland to arable land, therefore, should decrease the soils resilience to compaction and increase the susceptibility to compaction. The removal of the well developed dense root-zone created by perennial crops, mainly by grass, where a large number of small roots contributes more to the soil stabilization than a small number of large roots (Trükmann et al., 2009), may result in a reduction of the bearing capacity of the soil.

Soil organic matter is well known to play a crucial role in the soil's ability to withstand applied mechanical stresses; indirectly, by forming stable aggregates in conjunction with the soil mineral phase and by that, enhancing the structural stability of soils (Zhang and Hartge, 1990; Barral et al., 1998; Wiesmeier et al., 2012; Sandén et al., 2017). But also the sheer presence of unbound organic matter in the soil, contributing significantly to the soil's ability to absorb applied mechanical stresses in the form of elastic energy and release it after compaction as potential energy (McBride and Watson, 1990; Zhang et al., 2005), enables the soil to self-recover from compaction.

Several authors investigated the effect of tillage on different soil organic matter pools. Besnard et al. (1996), Six et al. (1998) and Chan (2001) revealed that tillage has a significant effect on soil organic matter. Especially the more labile particulate organic matter pools are affected to a greater extent by tillage and thus, eventually reducing the soil's resilience to compaction. Rising temperatures have a similar effect on the different soil organic matter pools than tillage. There is evidence that rising temperatures affect the particulate organic matter pools to a greater extent than the mineral-associated organic matter fractions (Kirschbaum, 1995; Zhang et al., 2007; Benbi et al., 2014). Both tillage and rising temperatures and especially the combination of both might, therefore, have critical negative repercussions on the soil mechanical properties.

In perspective of combined land-use change and climate change in the subarctic, the objective of this study was to compare the mechanical behaviour of pasture soils from South Greenland and cultivated typical soils from a temperate region. Uniaxial confined compression tests (UCCT) on 210 undisturbed soil core samples from three pasture fields in South Greenland and four cultivated areas across Denmark were carried out. The Danish soils were chosen to cover the ranges of textures and organic matter contents of the Greenlandic soils.

2. Material and Methods

2.1. Study sites and soil sampling

The three Greenlandic fields are located in southern Greenland, near the small settlement of South Igaliku (Igaliku Kujalleq), about 15 km south of Igaliku. Fields South-Igaliku 1 and South-Igaliku 2 (SI-1 and SI-2 respectively, N60°53′29.2″ W45°16′27.8″) are in direct proximity to the Einarsfjord (Igalikup Kangerlua), whereas field South-Igaliku 3 (SI-3, N60°51′39.1″ W45°16′26.4″) is located about 4.5 km in southern inland direction (Figure 1). The soils of SI-1 and SI-2 developed on granite (biotite- and hornblende bearing), overlain by aeolian and fluvial sands (Henriksen et al., 2009) and were classified as Arenic Umbrisols, according to IUSS Working Group WRB (2014). The soils of SI-3 developed on a mix of fluvial and aeolian sands originating form the deposition of the erosion belt created by the

tunnelled falling winds and the meltwater stream from the inland ice and was classified as an Loamic Umbrisol.

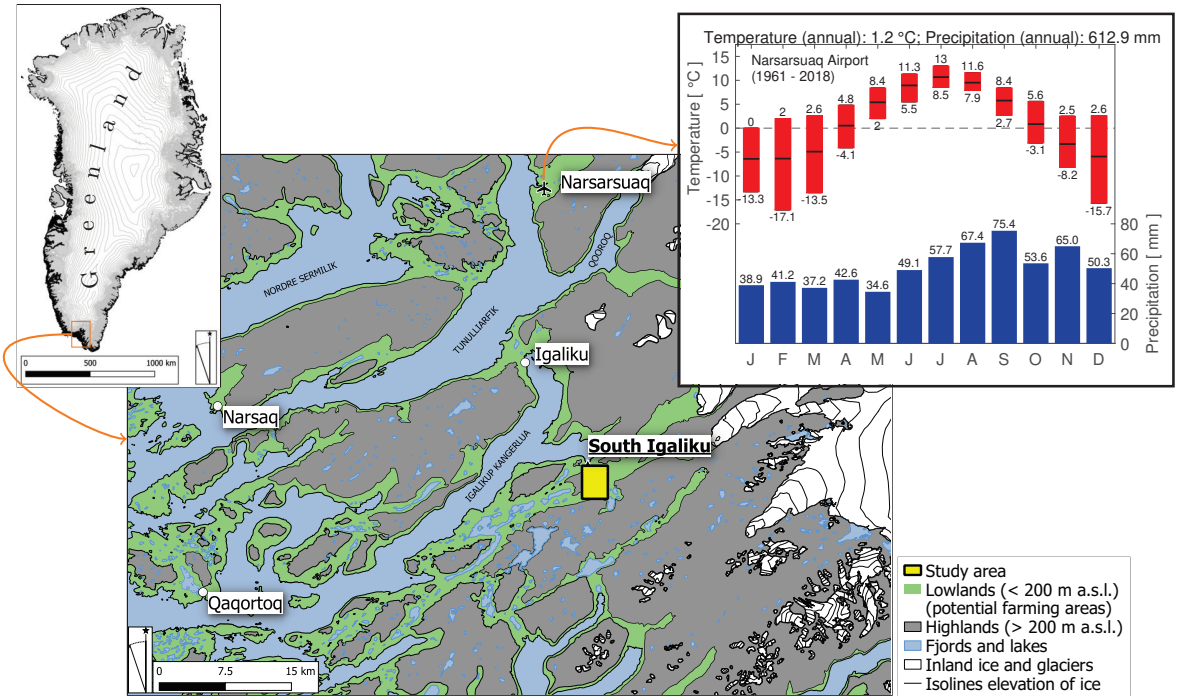

Figure 1: The study area indicated by the filled square, next to the small settlement of South Igaliku (Styrelsen for Dataforsyning og Effektivisering, 2018). Climate diagram for the climate station at Narsarsuaq airport (monthly averages from 1961 - 2018), extend of the boxes drawn for the temperature variation corresponds to the average minimum and maximum temperatures for the considered period, the black line represents the mean monthly temperature. (Cappelen, 2019).

Climate data showed an annual mean temperature of 1.2 °C with January being the coldest and July being the warmest moths with mean temperatures of -6.4 °C and 10.7 °C, respectively. The average total precipitation was 612.9 mm a^{-1} (Cappelen, 2008). The vegetation period only covers about three months considering the minimum average annual temperature for the considered period, assuming a minimum temperature of 3 °C necessary for plant growth (Inouye, 2000). Precipitation is highest in September with an average value of 75.4 mm and lowest in May with an average of 34.6 mm.

Fields SI-1 and SI-2 are used as pastures, mainly for sheep grazing during the summer months and have not been tilled recently. The third Greenlandic field, SI-3, has regularly (3-4 years interval) been cultivated (disc harrowed) since 1998 and is used as a forage grass source. Additionally, the area is drained by surface ditches, due to the proximity to a nearby stream, resulting in fairly different water availability conditions throughout the year, compared to the other two fields. Mineral fertiliser is applied once per year (early summer); the application of organic fertiliser is not a common practice in the region.

The sampling was carried out in August 2015, and all the three Greenlandic fields were sampled in regular grids, with 15×15 m for SI-1 and SI-3 and 7.5×7.5 m for SI-2. In total, 74 (32, 18 and 24 for SI-1, SI-2 and SI-3 respectively) undisturbed top-soil (10-20 cm depth) core samples (height 34.2 mm, inner diameter 60.1 mm, volume 100 cm^3) were collected with 2 replicates for each sampling point.

The Danish sampling sites are located throughout Jutland. From four differently textured agricultural fields, 62 undisturbed soil core samples between 10 to 20 cm depth with the same soil core dimensions as for the Greenlandic soils were collected during different sampling campaigns. All the Danish soils are from cultivated agricultural fields, subjected to conventional tillage.

The soil at the Jyndevad sampling site (N54°53′ E9°7′) developed on a fluvioglacial outwash plain of the Weichselian ice sheet (Lindhardt et al., 2001; Masís-Mendélez et al., 2014) and was classified as an Arenic Podzol (IUSS Working Group WRB , 2014). In total, 19 undisturbed soil core samples were

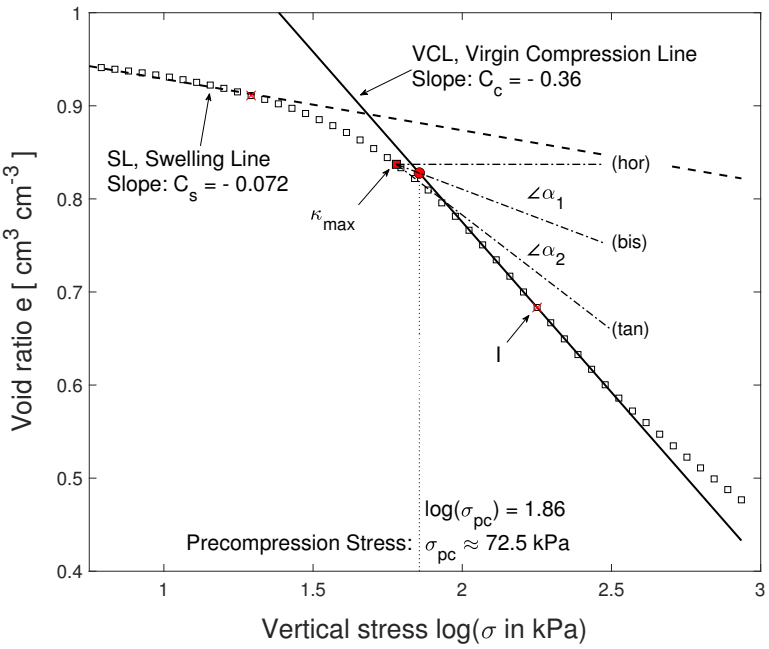

Figure 2: Obtaining the compression characteristics on the stress-void ratio curve: Compression index (C_c, kPa^{-1}), pre-compression stress (σ_{pc}, kPa) and swelling index (C_s, kPa^{-1}) from UCCT-experiments; σ_{pc} as proposed by Casagrande (1936) and following Gregory et al. (2006) and Keller et al. (2011) for C_c and C_s, respectively. Sample from Jyndevad as illustration. Table 1 lists the parameter explanation.

collected from this site. The soil at the Varde sampling site (N55°37′ E8°28′) developed on an eroded moraine landscape form the Saalian glaciation period with fluvioglacial and aeolian (loess) components from the Weichselian glaciation period. In total, 20 undisturbed soil core samples were collected from this site, classified as Arenic Podzol. The soil at the Estrup sampling site (N55°29′ E9°4′) developed on a moraine landscape from the Saale glaciation (Lindhardt et al., 2001; Paradelo et al., 2015) and was classified as Stagnic Podzol; in total, 16 undisturbed soil core samples were collected. The soil at the Odder sampling site (N55°58′ E10°6′) developed on moraine material from the last glaciation period (Weichsel glacial) and could be classified as Cambisol. From this site, seven undisturbed soil core samples were used.

The climate normals (1961-1991) for Denmark show an annual mean temperature of 7.7 °C with January being the coldest and July being the warmest months with mean temperatures of 0.0 °C and 15.7 °C, respectively. The annual average total precipitation for the mentioned period was 712mm a^{-1}, with a decline in total annual precipitation from west to east (823 to 584 mm a^{-1}, Cappelen, 2008).

In addition to the intact soil core samples, bulk soil was collected for each sampling point (Greenland and Denmark) for further analysis in the laboratory.

2.2. Methods

The mechanical properties of agricultural top-soils are often determined using uniaxial confined compression tests (UCCT), as the lateral confinement simulates quasi isotropic stress conditions (Lamandé et al., 2017). Depending on the purpose of the study, different loading times may be applied. For simulating traffic by agricultural machinery, where the duration of the stress application is generally less than one second (Keller and Lamandé, 2010), a strain-controlled, in contrast to a stress-controlled, compression test should be carried out.

The result of a UCC-tests is generally presented as a stress-deformation curve (Koolen, 1974). Expressed in a semi-logarithmic domain (stress, σ, in log-scale), an ideal compression curve can be divided into two regions, wherein each, the deformation follows a more or less linear path. Casagrande (1936) referred to it as a (bi-linear) elasto-plastic model: a linear elastic (reversible) deformation, described by the swelling or recompression line (SL) and a linear plastic (irreversible) deformation, represented by the virgin compression line (VCL) (Figure 2).

Table 1: Parameter explanation table for Figure 2. κ_{max} is the point of maximum curvature, and I is the inflection point of the $\log\sigma - \mathrm{e}$ curve for $\sigma > \sigma_{pc}$.

Stress - void ratio curve $\log(\sigma) - \mathrm{e}$ - graphical method				Figure 2
Symbol	Unit	Description	Formula/Relation	Reference
e	$\mathrm{cm}^3\,\mathrm{cm}^{-3}$	Void ratio	$\rho_s/\rho_b - 1$	Gupta et al. (2002)
σ_{pc}	kPa	Precompression stress	$VCL \cap$ bis	Casagrande (1936)
		hor: horizontal line passing through κ_{max} bis: bisector ($\angle\alpha_1 = \angle\alpha_2$) tan: tangent to κ_{max}		Dawidowski and Koolen (1994)
C_s	kPa^{-1}	Swelling / recompression index	$C_s = (\mathrm{e}_{1\,\mathrm{kPa}} - \mathrm{e}_{20\,\mathrm{kPa}})/\log(20\,\mathrm{kPa})$	Keller et al. (2011)
C_c	kPa^{-1}	Compression index	$C_c = \tan(I, \mathrm{e})$	Gregory et al. (2006)

The SL and VCL are connected by a transition point known as the precompression stress (or preconsolidation stress), σ_{pc}, first introduced by Casagrande (1936). It is a measure of the soil's maximum bearing capacity before irreversible deformation occurs within the soil (Lebert and Horn, 1991; Horn et al., 1995). Several methods to determine the soil's bearing capacity exist, including the graphical method introduced by (Casagrande, 1936), simple linear regressions (Junior and Pierce, 1995), fitting non-linear functions (Gregory et al., 2006) and numerical methods (Lamandé et al., 2017). Apart from the regression methods, σ_{pc} depends primarily on the point of maximum curvature, κ_{max}, of the compression curve.

Apart from σ_{pc}, three additional mechanical properties were considered in this study. The compression index, C_c, as the slope of the VCL, is a measure of the soil's susceptibility to compaction (compressibility) and describes the irreversible deformation of the soil during compaction (Imhoff et al., 2004). The swelling or recompression index, C_s, as the slope of the SL, is a measure of the soil's mechanical resilience (Stone and Larson, 1980), and following the ideal elasto-plastic model, the deformation described by C_s is reversible. Finally, the rebound, $\Delta\varepsilon$, as a measure of short term resilience or the soil's ability to recover from compaction. It was measured as the vertical expansion of the compacted soil sample, 60 seconds after the release of the applied normal load.

2.2.1. Uniaxial confined compression tests (UCCT) and rebound after compression.

Prior to the compression test, the samples were drained on a suction table to a soil water potential of $\psi = -100$ hPa (pF2), corresponding to the definition of the matric potential at field capacity for sandy soils (Al Majou et al., 2008)

A fully automated dual column table frame extensometer (Instron series 5960, Illinois Tool Works Inc.) was used to perform the UCC-tests. The device was mounted with a 5kN static load cell and a 59 mm i.d. compression piston. The test procedure consisted in a strain-controlled stress application with a constant strain rate of $1\,\mathrm{mm\,min}^{-1}$, as suggested by Koolen (1974) and Lamandé et al. (2017). The device's software recorded the displacement of the piston (extension in mm), positive in the downward direction, and the resulting load at the load cell (in N). The subsequent data analysis was entirely performed in the proprietary software MATLAB and Statistics Toolbox (2018).

The soil core sample was subjected to a small preload (5 N) to ensure full contact between piston and soil, and after balancing the load readings to zero, the actual compaction started together with the data recording. The test procedure was executed in several steps. The first step consisted in applying a normal stress to a maximum value of 800 kPa at a constant strain rate of $1\,\mathrm{mm\,min}^{-1}$. After the maximum value was reached, the piston retracted instantaneously to its initial position for a 60 sec waiting time. During this waiting time, hereafter relaxation time, the compacted soil was able to regain in volume (one-dimensional expansion in the vertical direction, rebound $\Delta\varepsilon$). The final step was then to determine the amount of the vertical expansion by measuring the difference between the extension at the maximum applied stress (800 kPa) and the extension after the relaxation time (60 sec). For this purpose, the cross-head moved down to the soil core cylinder again, and the displacement of the cylinder was recorded after preload (5 N). The simultaneous measurements of the applied normal load and compressive extension (d) were converted to applied vertical stress, σ (in kPa), and change in void ratio, e, according to equation (1),

$$e = (\rho_s/\rho_b)[(H-d)/H] - 1 \quad \text{and} \quad e_0 = [\rho_s/\rho_b] - 1 \tag{1}$$

with H being the initial height of the soil sample in the same unit as d, e_0 the initial void ratio and ρ_b and ρ_s the dry bulk and the average particle densities, respectively.

2.2.2. Numerical determination of the four mechanical parameters

The precompression stress, σ_{pc}, was determined using the graphical method introduced by Casagrande (1936), and its essential part is the determination of the point of maximum curvature (κ_{max}) of the compression curve. The numerical method recently introduced by Lamandé et al. (2017) is robust in finding κ_{max} without imposing a predefined shape on the stress-deformation curve and served as input for further calculations of the precompression stress via the Casagrande-method. The numerical method consists of fitting a polynomial of form $e = a \cdot (\log \sigma) + b \cdot (\log \sigma)^2$ to a neighbouring subset of equidistant points of the log(stress)-void ratio curve. The second derivative of a function is a measure for the degree of curvature of a continuous curve, and as the second derivative of the above equation is equal to $2b$, it immediately leads to the point of maximum curvature, which is at the point where b has its maximum. The minimum number of neighbouring points used for the fitting was determined by simultaneously finding the maximum of the coefficient of determination R^2 (close to 1) and a significance of the t-test (assessed by its p-value) of the regression coefficient b below 0.001 as a function of the number of pairs of stress-strain points that were included in the regression. A detailed description of the procedure can be found in Lamandé et al. (2017). This approach reduced the subjectivity of finding κ_{max} to a minimum compared to fitting (Arvidsson and Keller, 2004; Gregory et al., 2006) or even visual methods. The used procedure for finding the three lines needed for determining σ_{pc} followed Dawidowski and Koolen (1994).

The compression index, C_c, defined here as the slope of the tangent at the inflection point of the stress-void ratio curve (following Gregory et al., 2006, where C_c is given by the slope of the tangent at the inflection point of the fitted Gompertz-function), can also be determined using the numerical approach. Considering the applied polynomial for the local regressions and its second derivative, a necessary condition of a point to be an inflection point is that the second derivative at this point vanishes. Thus, finding the location where $b = 0$ at higher applied stresses than the precompression stress, gives a potential inflection point; the determination of the slope of its tangent is straightforward. The assumption that the necessary condition of the existence of an inflection point is also sufficient is valid in this case, because it is expected that the second derivative exists and changes sign at that point. If the second derivative does not vanish at any point right to κ_{max}, the slope of the tangent of the points where b is closest to zero is set as the compression index. In that case, the expression is reduced to the slope of the tangent of the compression curve at high applied loads. The advantage of this method compared to fitting methods is that no subjective assumptions about manually setting the reference points for linear regression are involved.

The swelling index, C_s, was calculated following Keller et al. (2011) as the average slope of the $\sigma - e$ curve between applied vertical stresses of 1 and 20 kPa. Keller et al. (2011) set the upper boundary for the determination of C_s to 25 kPa, in this study, however, it had to be lowered to 20 kPa as some of the determined precompression stresses were lower than 25 kPa (Jyndevad).

The rebound, $\Delta\varepsilon$, was calculated as the difference of the measured displacement of the cross-head from its initial position to the soil surface at an applied vertical stress of 800 kPa, d_{end} (end of compression) with the corresponding compressive strain $\varepsilon_{end} = d_{end}/H$ and the displacement to the soil sample's surface after a relaxation time of 60 sec without any applied vertical stress, d_{final} ($\varepsilon_{final} = d_{final}/H$). Thus the rebound expressed in unit strain equals: $\Delta\varepsilon = \varepsilon_{final} - \varepsilon_{end}$.

2.2.3. Supporting basic measurements

After the compression tests, the soil samples were oven-dried for 24 hours at 105 °C for dry bulk density (ρ_b) determination. The oven-dried samples were subsequently destroyed for a visual inspection of the presence and abundance of scarcely decomposed organic fragments.

On the air-dry and 2 mm pre-sieved bulk samples, the particle size distribution (PSD) was determined using wet sieving in combination with the hydrometer method, according to Gee and Or (2002). The total carbon content was determined using a LECO carbon analyser coupled to an infrared CO_2 Flash 2000 NC detector, and as the soils were free of carbonates, the organic carbon (OC) could be set equal to the total carbon content. The average particle density (ρ_s) of the Danish soils was estimated based on the gravimetric clay and organic matter contents, according to Schjønning et al. (2017), and

for the Greenlandic soils, ρ_s was measured by the water displacement method, according to Flint and Flint (2002).

2.3. Statistical Analysis

The relationships between the initial bulk density (ρ_b, independent variable, IV) and the soil mechanical properties (σ_{pc}, C_c, C_s and $\Delta\varepsilon$, dependent variables, DV) were investigated by linear regressions, if applicable. The goodness of fit of the linear regressions was quantified by the ordinary coefficient of determination, R^2, and the root mean square error, RMSE, calculated, according to Hollander et al. (2013). The level of significance was denoted by stars according to *** for $p < 0.001$, ** for $p < 0.01$, * for $p < 0.05$ and none for $p \geq 0.05$.

Pearson's linear correlation coefficient r was used to express the linear correlation between two variables (Hollander et al., 2013).

Box-whisker plots (Tukey, 1977) were used to visualise the relative differences or similarities between the measured mechanical parameters.

To test the land-use-specific difference in medians of the different soil mechanical parameters for significance, the Kruskal-Wallis test was used. It is a non-parametric method and does neither assume normally distributed observations, nor homoscedasticity and allows unbalanced datasets to test the hypothesis, that the medians of two groups come from the same distribution (Kruskal and Wallis, 1952). The result of the test was given by the χ^2-statistic and its p-value. If significant differences in values among the medians of the different groups were found, the Mann-Whitney-Wilcoxon U test (Mann and Whitney, 1947) served as the post-hoc test to identify the significance of the pairwise comparisons. The p-values were corrected for inflation of type I errors by using the Bonferroni method (Dunnett, 1955).

3. Results and Discussion

3.1. Texture, organic carbon contents and initial bulk densities

Table 2: Basic soil properties related to texture and structure of the soils used in this study. Median values of gravimetric fractions of clay (<2 µm), silt (2 - 50 µm) and sand (50 - 2000 µm) in $g\,g^{-1}$, organic carbon content (OC, $g\,g^{-1}$), average particle density (ρ_s, $g\,cm^{-3}$) and initial dry bulk density (ρ_b, $g\,cm^{-3}$). Clay-OC ratio Dexter n according to Dexter et al. (2008); N is the number of samples per site. Soil type according to Soil Survey Staff (1999) with S - Sand, lS - loamy Sand, sL - sandy Loam, L - Loam, cL - clay Loam. The figures in brackets denote the interquartile range (IQR = 75% quartile - 25% quartile). Medians in the same column bearing the same letter are not statistically different on a 5% significance level.

Data set / Site	N	Soil Type	Particle Size Distribution				Densities		Ratio
		USDA	Clay	Silt	Sand	OC	ρ_s	ρ_b	Dexter n
			$\times 10^{-2}$ [$g\,g^{-1}$]				[$g\,cm^{-3}$]		[-]
Greenlandic Soils (SI)	148		2.9 (1.2)	23.1 (3.5)	70.4 (4.4)	2.23 (1.51)	2.64 (0.04)	1.15 (0.23)	1.31 (0.38)
South-Igaliku 1 (SI-1)	64	lS-sL	2.9 (0.7)	22.4 (2.5)	71.4 (4.2)	2.09 (0.84)	2.64 (0.02)	1.12 (0.22)a	1.32 (0.38)
South-Igaliku 2 (SI-2)	36	lS-sL	2.2 (0.4)	23.8 (1.6)	71.6 (1.7)	1.45 (0.46)	2.66 (0.01)	1.27 (0.12)b	1.40 (0.78)
South-Igaliku 3 (SI-3)	48	lS-sL	4.1 (1.0)	24.1 (6.9)	65.3 (7.5)	3.13 (0.93)	2.62 (0.02)	1.08 (0.19)a	1.18 (0.40)
Danish Soils (DK)	62		5.7 (6.3)	16.8 (21.9)	73.4 (31.8)	2.18 (0.83)	2.58 (0.03)	1.43 (0.15)	2.52 (1.11)
Jyndevad	19	S	4.1 (0.5)	4.8 (0.4)	87.7 (1.0)	1.92 (0.27)	2.59 (0.01)	1.43 (0.07)c	2.16 (0.60)
Varde	20	lS-sL	5.3 (0.9)	16.6 (1.5)	73.6 (2.8)	2.29 (0.55)	2.58 (0.02)	1.44 (0.25)c	2.41 (0.64)
Estrup	16	sL-L	10.9 (2.0)	28.7 (2.5)	54.6 (3.9)	3.39 (2.87)	2.54 (0.12)	1.39 (0.27)c	3.12 (3.01)
Odder	7	sL-cL	16.0 (15.5)	26.7 (8.7)	54.6 (28.0)	1.57 (1.15)	2.62 (0.02)	1.52 (0.14)c	9.85 (0.64)

The soil type of the three Greenlandic fields ranged from sand to loamy sand, according to Soil Survey Staff (1999), with the dominant type being sandy loam (77% of the Greenlandic dataset). Average OC ranged between 0.0145 $g\,g^{-1}$ (SI-2) and 0.0313 $g\,g^{-1}$ (SI-3) with a median value of 0.0223 $g\,g^{-1}$ and clay contents ranging between 0.022 $g\,g^{-1}$ (SI-2) and 0.041 $g\,g^{-1}$ (SI-3) with a median value of 0.029 $g\,g^{-1}$. The site-specific basic soil properties are given in Table 2.

The soil types of the Danish soils were coarse sand (Jyndevad), loamy sand to sandy loam (Varde), sandy loam to loam (Estrup) and sandy loam to clay loam (Odder). The average OC contents of the Danish soils ranged from 0.0157 (Odder) to 0.0339 (Estrup) $g\,g^{-1}$, with Estrup exhibiting the highest variation in OC contents, see also Table 2.

Figure 3A shows a box-whisker plot of the gravimetric OC contents for all the soil used in this study. The chosen Danish arable fields covered the texture range of the Greenlandic ones (Figure 3B).

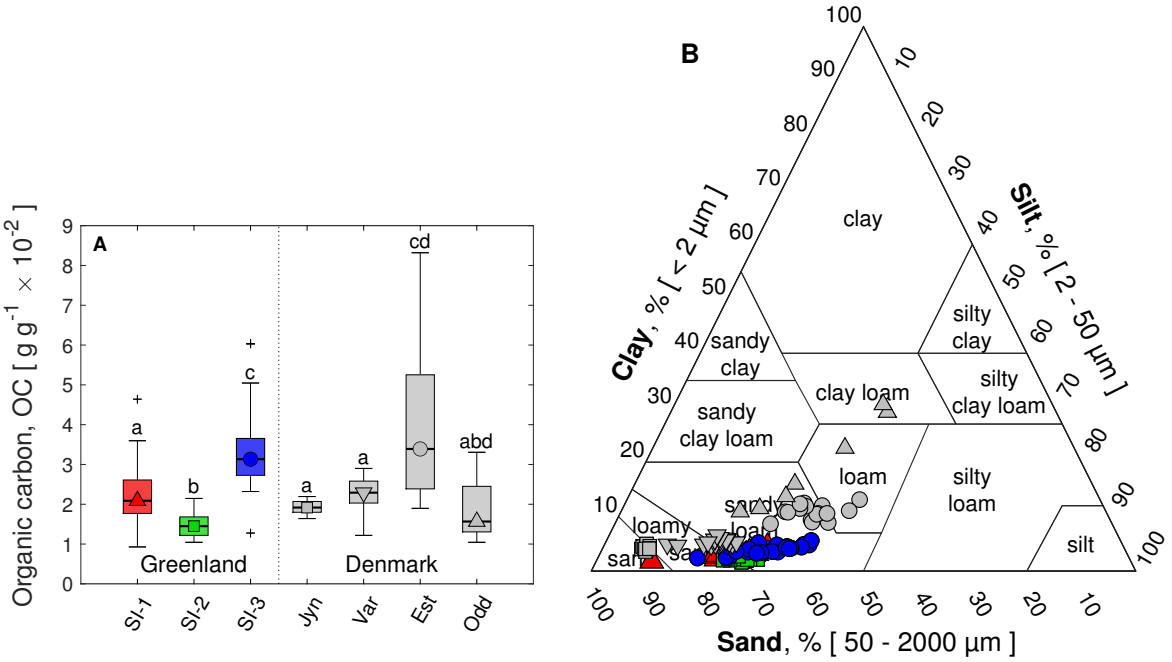

Figure 3: Texture and organic carbon contents of the soils used in this study. **A**; Box-whisker plot of the gravimetric organic carbon content (OC, $\mathrm{g\,g^{-1}}$). Columns bearing the same letters were not statistically different on a 5% significance level. The the horizontal line within the rectangular box represents the median value of each site, the upper and lower extension of the box depicts the first and third quartiles, respectively, and the whiskers extend to the minimum and maximum of the population cleared from outliers. Outliers are values that are more than three scaled median absolute deviations away from the population median (Rousseeuw and Croux, 1993) and depicted by black crosses. **B**; USDA soil texture triangle. Greenland: ▲ South-Igaliku 1 (SI-1), ■ South-Igaliku 2 (SI-2), ● South-Igaliku 3 (SI-3); Denmark: ▫ Jyndevad (Jyn), ○ Estrup (Est), ▽ Varde (Var) and △ Odder (Odd).

Among the Greenlandic dataset, SI-3 exhibited the highest OC and fine particle contents (particles with equivalent diameter < 50 µm).

Dexter et al. (2008) reported that the amount of complexed and non-complexed soil organic carbon contents play a crucial role in the soil's physical and functional behaviour. The clay-OC ratio for a given soil (Dexter n) should be below 10 to ensure that all the organic matter is bound to the clay minerals. For all the soils from Greenland, the majority of the organic carbon was not bound to the clay fraction due to the overabundance of organic material relative to the available surface area of the clay content (Dexter $n < 1.5$, cf. Table 2). Hence, relatively large amounts of non-complexed organic carbon were available within the soil matrix.

The visual examination of the sub-Arctic Greenlandic pasture soil samples revealed that they contained relatively large amounts of root and other scarcely decomposed plant litter fragments, in contrast to the Danish samples issued from permanently cultivated temperate lands. Although Dexter n of most of the Danish soils was well below ten (cf. Table 2), the absence of larger amounts of particulate organic matter was associated to the land-use and management (Chan, 2001; Ramesh et al., 2019), as well as to the enhanced organic matter turnover in temperate compared to subarctic environments (Benbi et al., 2014). The content of particulate organic matter was found to be positively correlated with soil stability and resilience to compaction (Bachmann and Zhang, 1991; Zhang et al., 2005). A reduction in particulate organic matter, therefore, should eventually lead to decreasing mechanical stability.

The initial dry bulk density, ρ_b, of the Greenlandic soils ranged between 1.08 and 1.27 $\mathrm{g\,cm^{-3}}$ (for SI-3 and SI-2, respectively, Table 2). Similar values for South Greenlandic pasture soils were found by Caviezel et al. (2017). The low values could partly be attributed to the high OC, showing a significant negative correlation (Greenland: $r = -0.74^{***}$, Denmark: $r = -0.54^{***}$) with ρ_b, as also reported in other studies (Gupta and Larson, 1979; Federer et al., 1993; Perie and Ouimet, 2008). A Kruskal-Wallis test indicated that ρ_b of the Greenlandic soils (mean rank $= 1.15$ $\mathrm{g\,cm^{-3}}$, $n = 148$) was statistically significantly lower than the ρ_b of the Danish dataset (mean rank $= 1.43$ $\mathrm{g\,cm^{-3}}$, $n = 62$),

$z = -9.45, p < 0.0001$.

The high OC content is, however, not the only factor affecting ρ_b of the Greenlandic soils. Among others, land-use influences ρ_b as other studies found lower ρ_b when comparing cultivated agricultural soils to perennial grasslands (Ajayi and Horn, 2016). Specific for the investigated region, temperature effects resulting in intense freeze and thaw cycles, leading to a high amount of voids in the soil matrix due to the expanding freezing water (Xie et al., 2015).

Table 3: Soil mechanical characteristics of the soils presented in this study. Median values of the precompression stress (σ_{pc}, kPa), the compression index (C_c, kPa^{-1}) and the swelling (recompression) index (C_s, kPa^{-1}) determined on the stress-void ratio curve ($\log\sigma$ - e), the rebound ($\Delta\varepsilon$, -) expressed in terms of unit strain and the recovery ($\Delta\rho$, %) expressed in percent of initial ρ_b. N is the number of samples per site. The figures in brackets denote the interquartile range (IQR = 75% quartile - 25% quartile). Medians in the same column bearing the same letter are not statistically different on a 5% significance level.

Data set / Site	N	σ_{pc}	C_c	C_s	$\Delta\varepsilon$	$\Delta\rho$
		[kPa]	$\times10^{-1}$ [kPa^{-1}]	$\times10^{-2}$ [kPa^{-1}]	$\times10^{-2}$ [-]	%
Greenlandic Soils (SI)	148	119.8 (55.6)	2.80 (1.77)	4.56 (3.03)	7.77 (3.56)	48.50 (6.66)
South-Igaliku 1 (SI-1)	64	125.2 (75.2)	3.10 (2.05)	4.60 (3.69)	7.94 (3.31)a	48.50 (5.90)
South-Igaliku 2 (SI-2)	36	115.5 (39.9)	1.96 (0.78)	3.59 (1.09)	5.67 (1.52)b	44.54 (4.69)
South-Igaliku 3 (SI-3)	48	114.7 (46.5)	3.19 (1.18)	5.64 (2.64)	9.14 (2.61)a	50.95 (6.82)
Danish Soils (DK)	62	75.6 (53.9)	1.73 (1.34)	3.66 (2.19)	5.23 (1.17)	35.64 (10.92)
Jyndevad	19	45.0 (32.3)	1.61 (0.26)	4.87 (1.34)	5.17 (0.59)b	27.28 (8.61)
Estrup	16	99.2 (100.7)	2.97 (0.96)	3.79 (1.64)	5.17 (1.01)b	35.40 (6.74)
Varde	20	88.5 (80.8)	1.18 (0.92)	2.83 (1.84)	5.80 (1.28)b	30.11 (14.69)
Odder	7	94.0 (29.3)	2.31 (1.27)	2.63 (1.09)	3.99 (2.43)b	41.75 (12.41)

3.2. Precompression stress

The field-specific average of the precompression stress, σ_{pc}, of the Greenlandic soils ranged between 114.7 (SI-3) and 125.2 (SI-1) kPa with an overall median of 119.8 kPa. The site-specific σ_{pc} are listed in Table 3. A Kruskal-Wallis test indicated that the σ_{pc} of the pooled Greenlandic soils (mean rank = 119.64 kPa, $n = 148$) were statistically significantly higher than the σ_{pc} of the pooled Danish dataset (mean rank = 71.74 kPa, $n = 62$), $\chi^2 = 27.15, p < 0.0001$. Figure 4A shows a box-whisker plot of σ_{pc} for the different sites, and following the pair-wise comparison test, only the samples from the Jyndevad site had significantly lower σ_{pc}.

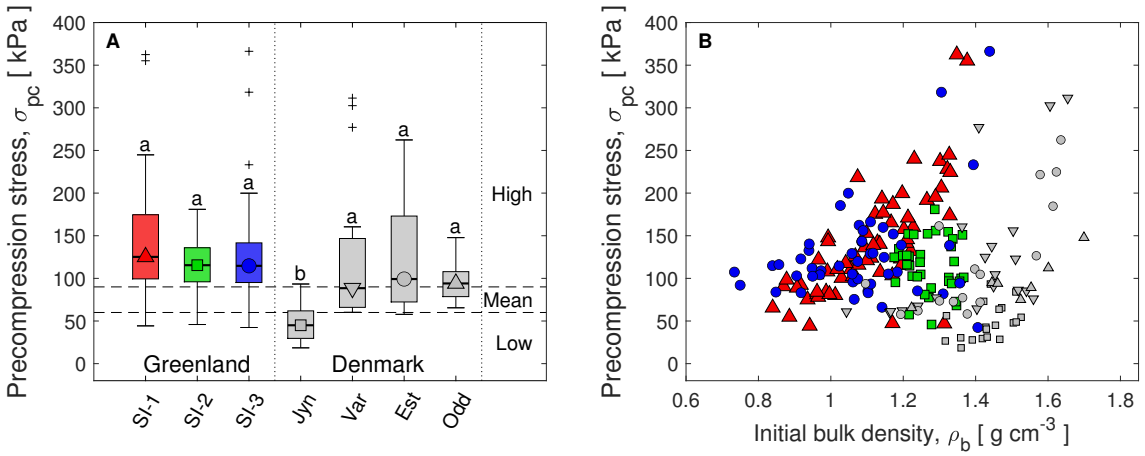

Figure 4: Precompression stress (σ_{pc}, kPa) as a measure of soil strength. **A**; Box-Whisker plot of σ_{pc} for the different sites, including levels of soil strength as proposed by Horn and Fleige (2003) marked by horizontal dashed lines. Columns bearing the same letters were not statistically different on a 5% significance level. **B**; σ_{pc} as a function of the initial bulk density (ρ_b, g cm^{-3}). Greenland: ▲ South-Igaliku 1 (SI-1), ■ South-Igaliku 2 (SI-2), ● South-Igaliku 3 (SI-3); Denmark: ▫ Jyndevad (Jyn), ○ Estrup (Est), ▽ Varde (Var) and △ Odder (Odd).

Following the classification for the bearing capacity of top-soils proposed by Horn and Fleige (2003), σ_{pc} of the three Greenlandic fields could be classified as *high*. Figure 4B shows the variation of σ_{pc}

with ρ_b and a slight positive tendency of σ_{pc} with increasing ρ_b can be observed; a significant linear correlation between the two variables could only be found for the samples from field SI-1 ($r = 0.74^{**}$).

A similar weak but significant positive correlation between σ_{pc} and ρ_b could be observed for the Danish cultivated soils ($r = 0.42^{***}$) what is in accordance to the findings of other studies (Salire et al., 1994; Rücknagel et al., 2007) investigating the mechanical soil properties of cultivated soils. Interestingly, despite having significantly lower ρ_b, the Greenlandic soils exhibited significantly higher σ_{pc} compared to those determined on the Danish soils as revealed above by the Wilcoxon ranked-sum test.

Figure 4B clearly shows that the dependence of σ_{pc} on ρ_b of the Greenlandic soils followed the same positive trend with increasing ρ_b as the Danish soils, but on a different level. Ajayi and Horn (2016) found an increased pore rigidity for soils under grassland compared to cultivated soils, which may affect the bearing capacity of the soil. The relatively large amounts of particulate organic matter and scarcely decomposed litter fragments found in the Greenlandic soils (cf section 3.1) may be partly responsible for the significantly higher σ_{pc}. Omitting the soils from Jyndevad from the Danish dataset, the remaining soils (Varde, Estrup and Odder) showed no statistically significant differences in σ_{pc}, but still, the Greenlandic soils showed significantly lower ρ_b (cf. Table 2). This indicated that the pore rigidity due to the plant cover (grass) and the soil-matrix elasticity provided by the unbound organic fragments, both missing in the Danish soils, had a significant positive effect on the Greenlandic soil's strength.

3.3. Compression index

Field-specific average C_c of the Greenlandic soils ranged between 0.196 (SI-2) and 0.319 (SI-3) kPa^{-1} with an overall median of 0.280 kPa^{-1} (absolute values). The site specific C_c are listed in Table 3. Figure 5A shows a box-whisker plot of C_c for the different sites. The pair-wise comparison test revealed that SI-2 exhibited significantly lower C_c than the other two Greenlandic fields.

Good agreements between the determination of C_c using the methods described in Gregory et al. (2006) or Keller et al. (2011) (tangent at the inflection point of the fitted Gompertz function to the stress-void ratio curve) and the method used in this study ($r = 0.92^{***}$, data not shown).

The linear correlation of the Greenlandic C_c (dependent variable, DV) with ρ_b (independent variable, IV) could be described by a significant linear regression with excellent goodness of fit given in equation (2).

$$\begin{aligned} C_c &= 1.22^{***} - 0.81^{***} \times \rho_b; \\ (RMSE &= 0.04; \quad R^2 = 0.92) \end{aligned} \tag{2}$$

where ρ_b is in $g\,cm^{-3}$.

Several other studies reported a linear dependence of C_c on ρ_b or on the initial void ratio (e_0) (Salire et al., 1994; Keller et al., 2011). The Danish soils followed a linear trend, exhibiting a considerably lower slope, as can be seen in Figure 5B. The regression equation determined for the C_c of the Danish soils ($C_c = 0.79 - 0.41 \times \rho_b$) was similar to the findings of Salire et al. (1994), $C_c = 0.89 - 0.44 \times \rho_b$; the goodness of fit and the significance levels were omitted due to the high degree of heteroscedasticity.

Higher C_c values indicated that the considered soil changed its volume to a larger extend for a given applied load. The low ρ_b resulted in a large amount of void space in the soil matrix. The irreversible reduction in volume at field conditions and relatively small applied stresses compared to the maximum applied stress during the UCCT (800 kPa) was mainly attributed to a reduction in the macro-porosity (Pagliai et al., 2003; Schäffer et al., 2007) and thus affecting soil aeration and hydraulic conductivity (Ahuja et al., 1984; Heard et al., 1988; Moldrup et al., 2001). Although the aggregate stability was not measured, the relatively low clay contents of the Greenlandic soils, as well as the intense freeze and thaw cycles in the region of interest, result in low aggregate stability (Lehrsch et al., 1991; Oztas and Fayetorbay, 2003) and once the bearing capacity of the top-soil overcome, the sandy Greenlandic soils are easily compacted.

3.4. Swelling index

Field-specific average C_s of the Greenlandic soils ranged between 3.59×10^{-2} kPa^{-1} (SI-2) and 5.64×10^{-2} kPa^{-1} (SI-3) kPa^{-1} with an overall median of 4.56×10^{-2} kPa^{-1} (absolute values). The

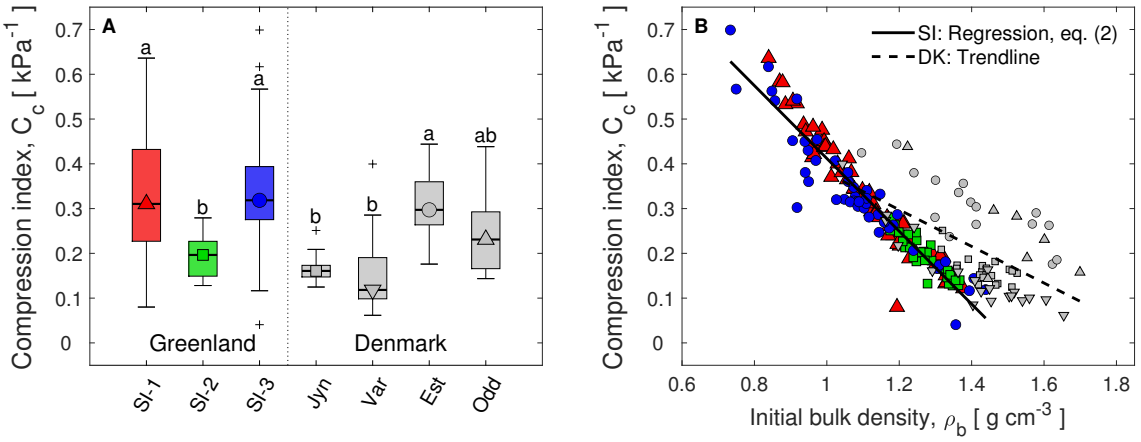

Figure 5: Compression index (C_c, kPa^{-1}) as a measure of compressibility. **A**; Box-whisker plot of C_c. Columns bearing the same letter are not statistically different on a 5% significance level. **B**; C_c as a function of the initial bulk density (ρ_b, g cm^{-3}). Solid regression line describes the trend of C_c of the Greenlandic soils (SI) with ρ_b as the independent variable; the dashed trend line shows the same for the Danish soils (DK). Greenland: ▲ South-Igaliku 1 (SI-1), ■ South-Igaliku 2 (SI-2), ● South-Igaliku 3 (SI-3); Denmark: ■ Jyndevad (Jyn), ● Estrup (Est), ▽ Varde (Var) and △ Odder (Odd).

site-specific C_s are listed in Table 3, and Figure 6A shows a box-whisker plot of C_s for the different sites. The variation of C_s with ρ_b of the complete dataset (SI + DK) could be best explained by a reciprocal relation; it is given in equation (3).

$$\begin{aligned} &C_s = 0.03^{***} / (\rho_b - 0.52^{***}); \\ &(\mathrm{RMSE} = 0.01; \quad R^2 = 0.64) \end{aligned} \tag{3}$$

where ρ_b is in g cm^{-3}. The lowest ρ_b exhibited the highest C_s, and the reciprocal nature of the relationship indicated a relatively abrupt change in the magnitude of C_s (decrease), once a certain ρ_b was exceeded.

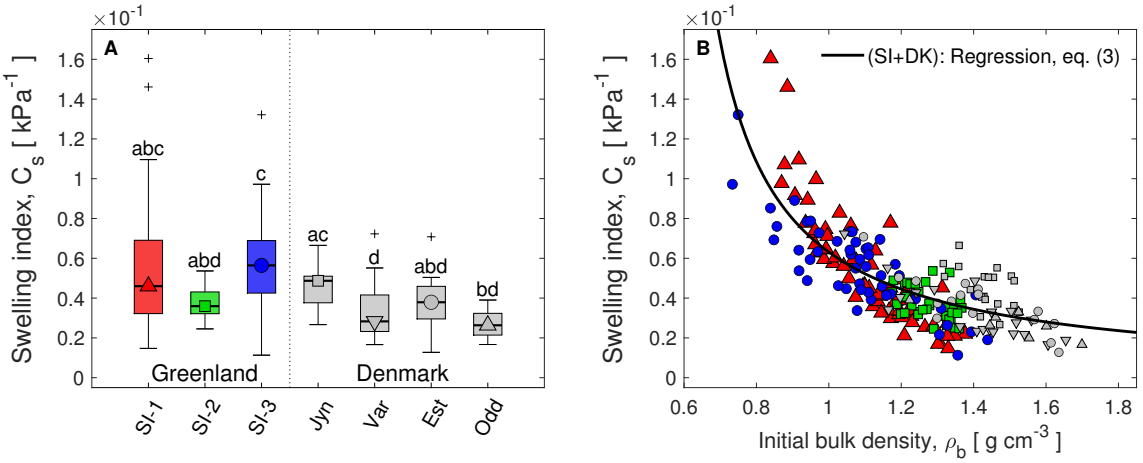

Figure 6: The swelling index (C_s,kPa^{-1}) as a measure of resilience to compaction. **A**; Box-whisker plot of C_s. Columns bearing the same letter are not statistically different on a 5% significance level. **B**; C_s versus the initial bulk density (ρ_b, kPa^{-1}) and a regression line showing the reciprocal correlation of C_s with ρ_b, valid for both datasets (SI + DK). Greenland: ▲ South-Igaliku 1 (SI-1), ■ South-Igaliku 2 (SI-2), ● South-Igaliku 3 (SI-3); Denmark: ■ Jyndevad (Jyn), ● Estrup (Est), ▽ Varde (Var) and △ Odder (Odd).

The Danish soils generally exhibited lower C_s than the Greenlandic soils, and a Kruskal-Wallis test indicated that the C_s of the Greenlandic soils (mean rank = 116.03, $n = 148$) were statistically significantly higher than the C_s of the Danish dataset (mean rank = 80.35, $n = 62$), $\chi^2 = 15.06, p <$

0.0001. Following the assumptions of the elasto-plastic model, the Greenlandic soils were more resilient to compaction than the Danish cultivated soils. This is in accordance with several other studies (Gregory et al., 2009; Dörner et al., 2011) in which pasture soils of temperate regions showed higher resilience to compaction than regularly tilled soils.

A significant positive correlation could be found between C_c and C_s ($r = 0.80^{***}$), with C_c being approximately six times higher than C_s ($C_c = 6.26\,(1.73) \times C_s$, figure in brackets denotes the interquartile range) for all the soils considered in this study clearly showing that the elastic behaviour was closely linked to the plastic deformation and did not consist of two separated events, as already pointed out by other authors (Keller et al., 2004). During the relatively fast compaction procedure used in this study, the redistribution of soil water needed to overcome the hydraulic impedance of the soil matrix, leading to reduced effective stress (Terzaghi, 1925) on the soil skeleton and thus to less plastic deformation and particle rearrangements. This may be one reason for the high correlation between C_c and C_s, meaning that the resilience to compaction (i.e., the elastic energy stored in the soil matrix) persisted, although the σ_{pc} was well exceeded.

3.5. Rebound

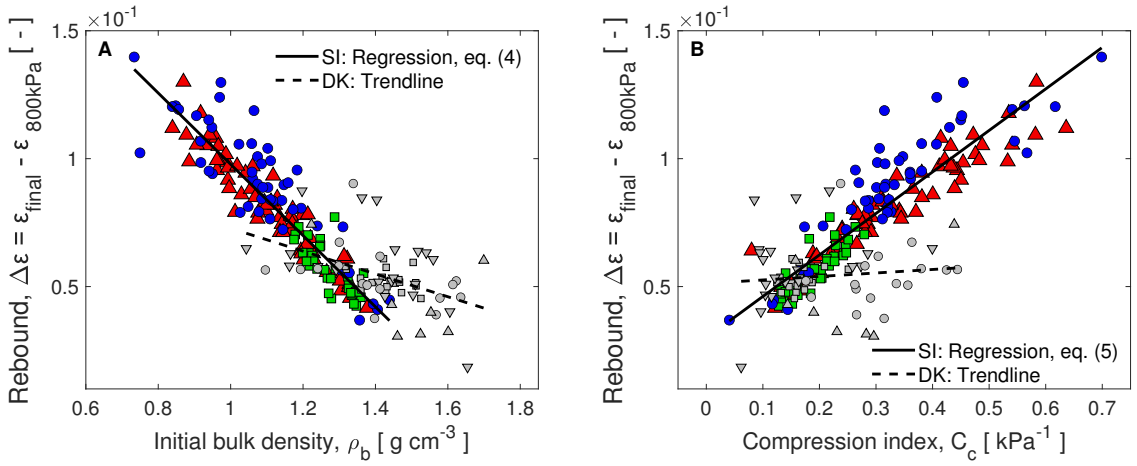

Figure 7: The rebound ($\Delta\varepsilon$, -) expressed in terms of compressive strain as a measure of short term recovery from compaction. **A**; $\Delta\varepsilon$ as a function of the initial bulk density (ρ_{b}, $\mathrm{g\,cm^{-3}}$) and the corresponding linear regression for the Greenlandic data (SI); the dashed line shows the general trend of the Danish dataset. **B**; $\Delta\varepsilon$ versus the compression index (C_{c}, $\mathrm{kPa^{-1}}$) and a linear regression for the Greenlandic data (SI); the dashed line shows the trend for the Danish dataset. Greenland: ▲ South-Igaliku 1 (SI-1), ■ South-Igaliku 2 (SI-2), ● South-Igaliku 3 (SI-3); Denmark: ▫ Jyndevad (Jyn), ○ Estrup (Est), ▽ Varde (Var) and △ Odder (Odd).

Field-specific average $\Delta\varepsilon$ of the Greenlandic soils ranged between 5.67×10^{-2} (SI-2) and 9.14×10^{-2} (SI-3) with an overall median of 7.77×10^{-2} units of strain. All the site-specific $\Delta\varepsilon$ are listed in Table 3. The Greenlandic soils exhibited generally higher $\Delta\varepsilon$ than the Danish soils, and a Kruskal-Wallis test confirmed that the $\Delta\varepsilon$ of the Greenlandic soils (mean rank = 124.20, $n = 148$) were statistically significantly higher than the $\Delta\varepsilon$ of the Danish dataset (mean rank = 60.87, $n = 62$), $\chi^2 = 47.45, p < 0.0001$.

Figure 7A shows the linear relation between $\Delta\varepsilon$ and ρ_{b} for the Greenlandic soils given in equation (4), exhibiting markedly higher intercept and slope than the shown trend-line of the Danish cultivated soils.

$$\begin{aligned} &\Delta\varepsilon = 0.24^{***} - 0.14^{***} \times \rho_{\mathrm{b}}; \\ &(\mathrm{RMSE} = 0.01; \quad \mathrm{R}^2 = 0.85) \end{aligned} \tag{4}$$

where ρ_{b} is in $\mathrm{g\,cm^{-3}}$. The most intuitive explanation and reason for the higher $\Delta\varepsilon$ of the Greenlandic soils are their significantly lower ρ_{b}. A less-dense soil needs less energy input to be moved, disregarding the direction of the movement, but the lower ρ_{b} might not be the only reason. Zhang et al. (2005) reported that high organic matter contents increased the rigidity of pores and that a large amount of

particulate organic matter would act as a spring. The relatively high amounts of particulate organic matter present in the Greenlandic pasture soils could, therefore, be partly responsible for the relatively high measured rebound.

It is not completely clear what caused the higher $\Delta\varepsilon$ of the Greenlandic pasture soils specifically, as hydraulic parameters like the soil water potential were not monitored or controlled during the compression tests. Measurements of the saturated hydraulic conductivity were low for the Greenlandic soils (data not shown), despite their high total porosity (data not shown) what might indicate the presence of dead-end pores, resulting in entrapped air pockets contributing to a larger rebound after the release of the stress.

Figure 7B shows the relation between $\Delta\varepsilon$ and C_c. A significant linear regression could be found for the Greenlandic soils, given in equation (5), whereas the Danish cultivated soils showed only marginal sensitivity to C_c.

$$\begin{aligned} \Delta\varepsilon &= 0.03^{***} + 0.16^{***} \times C_c; \\ (\mathrm{RMSE} &= 0.01; \quad \mathrm{R}^2 = 0.83) \end{aligned} \tag{5}$$

where C_c is in kPa^{-1}. This suggests that the mechanisms involved in the relaxation after compression were of different nature for the soils from two different land uses and climatic regions.

3.6. Bulk densities during compression and recovery potential after compression

In the following, ρ_b and changes in ρ_b due to compression were used instead of e_0 and changes in e, because all of those parameters were directly measured or calculated and not estimated from other parameters, reducing the risk of introducing artefacts in the shown relations. The rebound, technically not being a level of compaction as no stress is applied to the soil, was included in the terms levels or degrees of compaction for better legibility.

The bulk densities at 800 kPa ($\rho_{b,800\,kPa}$) and after rebound ($\rho_{b,\Delta\varepsilon}$) as a function of the initial bulk density ρ_b are presented in Figure 8A. To improve readability, only every third data-point was plotted. The $\rho_{b,m}$ at the two levels of compaction, were calculated via the compressive strain, ε, and ρ_b, according to equation 6.

$$\rho_{b,m} = \rho_b[1/(1-\varepsilon_m)] \tag{6}$$

where m denotes a given compaction level. Examination of ρ_b at the two levels of compaction revealed that the relationship was best described by including the squared initial ρ_b as IV in the regression. Hence, the complete dataset could be adequately described by one regression for each of the two compaction levels (equations (7) and (8)).

$$\begin{aligned} \rho_{b,800kPa} &= 0.90^{***} + 0.39^{***} \times (\rho_b)^2; \\ (\mathrm{RMSE} &= 0.07; \quad \mathrm{R}^2 = 0.87) \end{aligned} \tag{7}$$

$$\begin{aligned} \rho_{b,\Delta\varepsilon} &= 0.71^{**} + 0.43^{***} \times (\rho_b)^2; \\ (\mathrm{RMSE} &= 0.06; \quad \mathrm{R}^2 = 0.91) \end{aligned} \tag{8}$$

where ρ_b is in $\mathrm{g\,cm}^{-3}$.

For the given data, the plotted regression lines (Figure 8A) approached each other with increasing ρ_b; the difference between $\rho_{b,800kPa}$ and $\rho_{b,\Delta\varepsilon}$ decreased with increasing initial ρ_b. This vertical distance between the two lines is a measure of how much a soil sample can recover from compaction.

Figure 8B shows to what extent the different sites were able to recover from $\rho_{b,800kPa}$ back towards their initial bulk densities (ρ_b). By taking the ratio, $\Delta\rho$ = [$\rho_{b,800kPa}$ - $\rho_{b,\Delta\varepsilon}$] / [$\rho_{b,800kPa}$ - ρ_b], the effect of the significantly lower initial bulk density of the Greenlandic pasture soils could be eliminated. According to a Kruskal-Wallis test, $\Delta\rho$ of the Greenlandic soils (mean rank = 128.56, n = 148) was statistically significantly higher than $\Delta\rho_b$ of the Danish soils (mean rank = 50.45, n = 62), χ^2 = 72.19, $p < 0.0001$. The site-specific values of $\Delta\rho$ are given in Table 3. The values of recovery were very high in this study compared to other studies (Stone and Larson, 1980; Keller et al., 2011). This differences can be explained by that the Stone and Larson and Keller et al. studies used a sequential

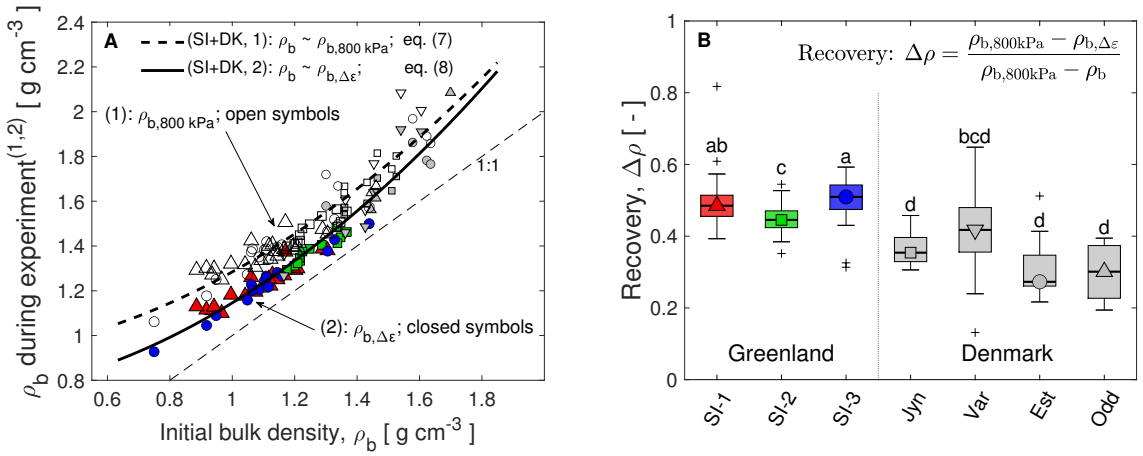

Figure 8: Bulk density history at different stages (1 and 2) of the compression experiment. **A**; ρ_b at a normal stress of 800 kPa (1, open symbols; $\rho_{b,800kPa}$, g cm^{-3}) and after the relaxation time (2, closed coloured symbols; $\rho_{b,\Delta\varepsilon}$, g cm^{-3}) as a function of ρ_b. The 1:1 line represents the initial ρ_b. Data reduced for better legibility (each third point). **B**; Recovery ($\Delta\rho_b$, -), defined as the ability of a sample to return to its initial ρ_b during the relaxation time. Columns bearing the same letters are not statistically different on a 5% significance level. Greenland: ▲ South-Igaliku 1 (SI-1), ■ South-Igaliku 2 (SI-2), ● South-Igaliku 3 (SI-3); Denmark: ■ Jyndevad (Jyn), ● Estrup (Est), ▽ Varde (Var) and △ Odder (Odd).

loading procedure with relatively long loading times, in contrast to the relatively fast strain-controlled procedure used in this study (Ghezzehei and Or, 2001).

Interestingly, among the Danish soils, Varde exhibited the highest recovery potential (not significantly different from SI-1 and SI-2), and it shared the most similar particle size distribution and similar OC content with the Greenlandic soils. This indicates that the recovery potential is dependent on both soil texture and OC, although it was not possible to find a simple statistically significant relationship between the three parameters for the used dataset.

4. Conclusion

The Greenlandic pasture soils exhibited significantly higher precompression stress, σ_{pc}, than the Danish cultivated soils despite markedly lower initial bulk densities, ρ_b. A main reason for the higher σ_{pc} of the Greenlandic soil is likely a large amount of non-complexed, particulate organic matter in the soil matrix. For some of the Greenlandic soils, a significant positive correlation between ρ_b and σ_{pc} could be found ($r = 0.74$).

The compression indices, C_c, of the Greenlandic pasture soils were significantly higher than for the Danish cultivated soils, and lower ρ_b gave higher C_c, likely due to a relatively large volume of easily compressible void space in the soil matrix. A strong linear relation between ρ_b and C_c for the Greenlandic soils was found ($R^2 = 0.92$).

The swelling indices, C_s, of the Greenlandic soils were also significantly higher than for the Danish soils. Lower ρ_b gave higher C_s due to increased pore rigidity and the relatively large amounts of particulate organic matter stemming from the permanent soil cover (grass). A reciprocal relation for the pooled (Greenlandic and Danish) dataset between ρ_b and C_s was found ($R^2 = 0.64$).

The rebound in terms of unit strain, $\Delta\varepsilon$, of the Greenlandic soils was significantly higher than the $\Delta\varepsilon$ of the Danish cultivated soils. The Greenlandic $\Delta\varepsilon$ showed a significant negative linear dependence on ρ_b ($R^2 = 0.85$). The recovery in terms of % of initial ρ_b, $\Delta\rho$, showed that the Greenlandic pasture soils could recover significantly better from severe compaction than the Danish cultivated soils.

For the Greenlandic pasture soils, the initial bulk density was overall a good predictor for all the mechanical properties considered in this study. Differences to Danish cultivated soils were associated with nature of the organic matter (particulate organic matter in the arctic pasture/grassland soils) and low bulk densities.

In perspective, a future land-use change from pasture to more intense cultivation together with rising temperatures in South Greenland would result in a reduction of particulate organic matter

and thereby decrease the σ_{pc} of the sandy Greenlandic soils. The low clay contents, together with a reduction in organic matter, could further result in a weakly structured soil matrix, and the present high resilience and recovery potential to compaction would decline.

Acknowledgements

This research was financed by the Danish Council for Independent Research, Technology and Production Sciences via the project: Glacial flour as a new, climate-positive technology for sustainable agriculture in Greenland: NewLand.

References

Ahuja, L. R., Naney, J. W., Green, R. E., Nielsen, D. R., 1984. Macroporosity to characterize spatial variability of hydraulic conductivity and effects of land management. Soil Sci. Soc. Am. J. 48 (4), 699–702.

Ajayi, A. E., Horn, R., 2016. Transformation of ex-arable land to permanent grassland promotes pore rigidity and mechanical soil resilience. Ecol. Eng. 94, 592–598.

Al Majou, H., Bruand, A., Duval, O., 2008. Use of in situ volumetric water content to improve prediction of soil water retention properties. Can. J. Soil Sci. 88, 533–541.

Alakukku, L., Elonen, P., 1995. Long-term effects of a single compaction by heavy field traffic on yield and nitrogen uptake of annual crops. Soil Tillage Res. 36 (3), 141–152.

Arvidsson, J., Keller, T., 2004. Soil precompression stress: I. A survey of Swedish arable soils. Soil Tillage Res. 77 (1), 85–95.

Austrheim, G., Asheim, L., Bjarnason, G., Feilberg, J., Fosaa, A. M., Holand, O., Høegh, K., Jónsdóttir, I., Magnusson, B., Mortensen, L., Mysterud, A., Olsen, E., Skonhoft, A., Steinheim, G., Thorhallsdottir, A., 2008. Sheep grazing in the North Atlantic region: A long term perspective on management, resource economy and ecology. Rapport Zoology Series 3, 1–82.

Bachmann, J., Zhang, H., 1991. Die Stabilität von Sandböden in Abhängigkeit vom Gehalt an organischer Substanz und deren Humifizierungsgrad. Zeitschrift für Pflanzenernährung und Bodenkunde 154 (1), 47–52.

Barral, M. T., Arias, M., Guérif, J., 1998. Effects of iron and organic matter on the porosity and structural stability of soil aggregates. Soil Tillage Res. 46 (3), 261–272.

Benbi, D. K., Boparai, A. K., Brar, K., 2014. Decomposition of particulate organic matter is more sensitive to temperature than the mineral associated organic matter. Soil Biol. Biochem. 70, 183–192.

Besnard, E., Chenu, C., Balesdent, J., Puget, P., Arrouyas, D., 1996. Fate of particulate organic matter in soil aggregates during cultivation. Eur. J. Soil Sci. 47 (4), 495–503.

Beylich, A., Oberholzer, H.-R., Schrader, S., Höper, H., Wilke, B.-M., 2010. Evaluation of soil compaction effects on soil biota and soil biological processes in soils. Soil Tillage Res. 109 (2), 133–143.

Cappelen, J., 2008. Guide to climate data and information from the Danish Meteorological Institute. Tech. Rep. 12-08, DMI, Danish Meteorological Institute, Copenhagen, from http://www.dmi.dk/dmi/tr12-08 (visited online: March 24, 2021).

Cappelen, J., 2019. Guide to climate data and information from the Danish Meteorological Institute. Tech. Rep. 19-10, DMI, Danish Meteorological Institute, Copenhagen, from http://www.dmi.dk/dmi/tr19-10 (visited online: March 24, 2021).

Casagrande, A., 1936. The determination of pre-consolidation load and its practical significance. In: Proceedings of the First International Conference on Soil Mechanics and Foundation Engineering. Vol. 3. Harvard University, Cambridge, MA, USA, pp. 60–64.

Caviezel, C., Hunziker, M., Kuhn, N. J., 2017. Bequest of the Norseman—The potential for agricultural intensification and expansion in southern Greenland under climate change. Land 6 (4), 1–20.

Chan, K. Y., 2001. Soil particulate organic carbon under different land use and management. Soil Use Manage. 17 (4), 217–221.

Dawidowski, J. B., Koolen, A. J., 1994. Computerized determination of the preconsolidation stress in compaction testing of field core samples. Soil Tillage Res. 31 (2), 277–282.

Dexter, A. R., Richard, G., Arrouays, D., Czyż, E. A., Jolivet, C., Duval, O., 2008. Complexed organic matter controls soil physical properties. Geoderma 144 (3), 620–627.

Dörner, J., Dec, D., Zúñiga, F., Sandoval, P., Horn, R., 2011. Effect of land use change on Andosol's pore functions and their functional resilience after mechanical and hydraulic stresses. Soil Tillage Res. 115-116, 71–79.

Dunnett, C. W., 1955. A multiple comparison procedure for comparing several treatments with a control. J. Am. Stat. Assoc. 50 (272), 1096–1121.

Federer, C. A., Turcotte, D. E., Smith, C. T., 1993. The organic fraction–bulk density relationship and the expression of nutrient content in forest soils. Can. J. For. Res. 23 (6), 1026–1032.

Flint, L. E., Flint, A. L., 2002. Particle density. In: Dane, J. H., Topp, G. C. (Eds.), Methods of Soil Analysis: Part 4 Physical Methods. Vol. 4 of 5. SSSA Book Series, Madison, Wisconsin, Ch. 2.2, pp. 229–240.

Gee, G. W., Or, D., 2002. Particle-size analysis. In: Dane, J. H., Topp, G. C. (Eds.), Methods of Soil Analysis: Part 4 Physical Methods. Vol. 4 of 5. SSSA Book Series, Madison, Wisconsin, Ch. 2.4, pp. 255–293.

Ghezzehei, T. A., Or, D., 2001. Rheological properties of wet soils and clays under steady and oscillatory stresses. Soil Sci. Soc. Am. J. 65 (3), 624–637.

Gregory, A. S., Watts, C. W., Griffiths, B. S., Hallett, P. D., Kuan, H. L., Whitmore, A. P., 2009. The effect of long-term soil management on the physical and biological resilience of a range of arable and grassland soils in England. Geoderma 153 (1), 172–185.

Gregory, A. S., Whalley, W. R., Watts, C. W., Bird, N. R. A., Hallett, P. D., Whitmore, A. P., 2006. Calculation of the compression index and precompression stress from soil compression test data. Soil Tillage Res. 89 (1), 45–57.

Gupta, S. C., Bradford, J. M., Drescher, A., 2002. Soil compressibility. In: Dane, J. H., Topp, G. C. (Eds.), Methods of Soil Analysis: Part 4 Physical Methods. Vol. 4 of 5. SSSA Book Series, Madison, Wisconsin, Ch. 2.10, pp. 399–415.

Gupta, S. C., Larson, W. E., 1979. A model for predicting packing density of soils using particle-size distribution. Soil Sci. Soc. Am. J. 43 (4), 758–764.

Heard, J. R., Kladivko, E. J., Mannering, J. V., 1988. Soil macroporosity, hydraulic conductivity and air permeability of silty soils under long-term conservation tillage in Indiana. Soil Tillage Res. 11 (1), 1–18.

Henriksen, N. nad Higgins, A. K., Kalsbeek, F., Pulvertaft, T. C. R., 2009. Greenland from Archaean to Quaternary. Descriptive text to the 1995 Geological map of Greenland, 1:2 500 000. Geological Survey of Denmark and Greenland Bulletin 18, 126 pp. + map.

Håkansson, I., Voorhees, W. B., Riley, H., 1988. Vehicle and wheel factors influencing soil compaction and crop response in different traffic regimes. Soil Tillage Res. 11 (3), 239–282, proceedings 11th Conference of ISTRO: Tillage and Traffic in Crop Production.

Hollander, M., Wolfe, D. A., Chicken, E., 2013. Nonparametric statistical methods, 3rd Edition. Vol. 751. John Wiley & Sons, Hoboken, New Jersey.

Horn, R., 2003. Stress–strain effects in structured unsaturated soils on coupled mechanical and hydraulic processes. Geoderma 116 (1-2), 77–88.

Horn, R., Domżał, H., Słowińska-Jurkiewicz, A., van Ouwerkerk, C., 1995. Soil compaction processes and their effects on the structure of arable soils and the environment. Soil Tillage Res. 35 (1), 23–36.

Horn, R., Fleige, H., 2003. A method for assessing the impact of load on mechanical stability and on physical properties of soils. Soil Tillage Res. 73 (1-2), 89–99.

Imhoff, S., Da Silva, A. P., Fallow, D., 2004. Susceptibility to compaction, load support capacity, and soil compressibility of Hapludox. Soil Sci. Soc. Am. J. 68 (1), 17–24.

Inouye, D. W., 2000. The ecological and evolutionary significance of frost in the context of climate change. Ecol. Lett. 3 (5), 457–463.

Jacobsen, N. K., 1987. Studies on soils and potential for soil erosion in the sheep farming area of South Greenland. Arct. Alp. Res. 19 (4), 498–507.

Junior, M. S. D., Pierce, F. J., 1995. A simple procedure for estimating preconsolidation pressure from soil compression curves. Soil Technology 8 (2), 139–151.

Keller, T., Arvidsson, J., Dawidowski, J. B., Koolen, A. J., 2004. Soil precompression stress: II. A comparison of different compaction tests and stress–displacement behaviour of the soil during wheeling. Soil Tillage Res. 77 (1), 97–108.

Keller, T., Lamandé, M., 2010. Challenges in the development of analytical soil compaction models. Soil Tillage Res. 111 (1), 54–64.

Keller, T., Lamandé, M., Schjønning, P., Dexter, A. R., 2011. Analysis of soil compression curves from uniaxial confined compression tests. Geoderma 163 (1), 13–23.

Kirschbaum, M. U. F., 1995. The temperature dependence of soil organic matter decomposition, and the effect of global warming on soil organic C storage. Soil Biol. Biochem. 27 (6), 753–760.

Koolen, A. J., 1974. A method for soil compactibility determination. J. Agric. Eng. Res. 19 (3), 271–278.

Kruskal, W. H., Wallis, W. A., 1952. Use of ranks in one-criterion variance analysis. J. Am. Stat. Assoc. 47 (260), 583–621.

Lamandé, M., Schjønning, P., Labouriau, R., 2017. A novel method for estimating soil precompression stress from uniaxial confined compression tests. Soil Sci. Soc. Am. J. 81 (5), 1005–1013.

Lebert, M., Horn, R., 1991. A method to predict the mechanical strength of agricultural soils. Soil Tillage Res. 19 (2), 275–286.

Lehrsch, G. A., Sojka, R. E., Carter, D. L., Jolley, P. M., 1991. Freezing effects on aggregate stability affected by texture, mineralogy, and organic matter. Soil Sci. Soc. Am. J. 55 (5), 1401–1406.

Lindhardt, B., Abildtrup, C., Vosgerau, H., Olsen, P., Torp, S., Iversen, B. V., Jørgensen, J. O., Plauborg, F., Rasmussen, P., Gravesen, P., 2001. The Danish pesticide leaching assessment programme. Site characterization and monitoring design, GEUS, Copenhagen, Denmark.

Lipiec, J., Stepniewski, W., 1995. Effects of soil compaction and tillage systems on uptake and losses of nutrients. Soil Tillage Res. 35 (1), 37–52.

Mann, H. B., Whitney, D. R., 1947. On a test of whether one of two random variables is stochastically larger than the other. Ann. Math. Stat. 18 (1), 50–60.

Masís-Mendélez, F., Deepagoda, T. K. K. C., de Jonge, L. W., Tuller, M., Moldrup, P., 2014. Gas diffusion-derived tortuosity governs saturated hydraulic conductivity in sandy soils. J. Hydrol. 512, 388–396.

MATLAB and Statistics Toolbox, 2018. version 9.5.0 (R2018b). The MathWorks Inc., Natick, Massachusetts.

McBride, R. A., Watson, G. C., 1990. An investigation of the re-expansion of unsaturated, structured soils during cyclic static loading. Soil Tillage Res. 17 (3), 241–253.

Moldrup, P., Olesen, T., Komatsu, T., Schjønning, P., Rolston, D. E., 2001. Tortuosity, diffusivity, and permeability in the soil liquid and gaseous phases. Soil Sci. Soc. Am. J. 65 (3), 613–623.

Oztas, T., Fayetorbay, F., 2003. Effect of freezing and thawing processes on soil aggregate stability. Catena 52 (1), 1–8.

Pagliai, M., Marsili, A., Servadio, P., Vignozzi, N., Pellegrini, S., 2003. Changes in some physical properties of a clay soil in central Italy following the passage of rubber tracked and wheeled tractors of medium power. Soil Tillage Res. 73 (1), 119–129.

Paradelo, M., Norgaard, T., Moldrup, P., Ferré, T. P. A., Kumari, K. G. I. D., Arthur, E., de Jonge, L. W., 2015. Prediction of the glyphosate sorption coefficient across two loamy agricultural fields. Geoderma 259-260, 224–232.

Park, T., Ganguly, S., Tømmervik, H., Euskirchen, E. S., Høgda, K.-A., Karlsen, S. R., Brovkin, V., Nemani, R. R., Myneni, R. B., 2016. Changes in growing season duration and productivity of northern vegetation inferred from long-term remote sensing data. Environ. Res. Lett. 11 (8), 084001.

Perie, C., Ouimet, R., 2008. Organic carbon, organic matter and bulk density relationships in boreal forest soils. Can. J. Soil Sci. 88 (3), 315–325.

Peth, S., Horn, R., 2006. Consequences of grazing on soil physical and mechanical properties in forest and tundra environments. In: Forbes, B. C., Bölter, M., Müller-Wille, L., Hukkinen, J., Müller, F., Gunslay, N., Konstantinov, Y. (Eds.), Reindeer Management in Northernmost Europe: Linking Practical and Scientific Knowledge in Social-Ecological Systems. Vol. 184. Springer Berlin Heidelberg, Berlin, Heidelberg, Ch. 11, pp. 217–243.

Ramesh, T., Bolan, N. S., Kirkham, M. B., Wijesekara, H., Kanchikerimath, M., Rao, C. S., Sandeep, S., Rinklebe, J., Ok, Y. S., Choudhury, B. U., Wang, H., Tang, C., Wang, X., Song, Z., Freeman, O. W., 2019. Soil organic carbon dynamics: Impact of land use changes and management practices: A review. In: Sparks, D. L. (Ed.), Advances in Agronomy. Vol. 156 of Advances in Agronomy. Academic Press, Ch. 1, pp. 1–107.

Rücknagel, J., Hofmann, B., Paul, R., Christen, O., Hülsbergen, K.-J., 2007. Estimating precompression stress of structured soils on the basis of aggregate density and dry bulk density. Soil Tillage Res. 92 (1), 213–220.

Reykdal, l., Sveinsson, S., Dalmannsdóttir, S., Martin, P., í Gerðinum, J. I., Kavanagh, V., Frederiksen, A., Hermannsson, J., Apr. 2016. Northern cereals – New opportunities. Final report, NORA.

Rousseeuw, P. J., Croux, C., 1993. Alternatives to the median absolute deviation. J. Am. Stat. Assoc. 88 (424), 1273–1283.

Salire, E. V., Hammel, J. E., Hardcastle, J. H., 1994. Compression of intact subsoils under short-duration loading. Soil Tillage Res. 31 (2), 235–248.

Sandén, T., Lair, G. J., Van Leeuwen, J. P., Gísladóttir, G., Bloem, J., Ragnarsdóttir, K. V., Steffens, M., Blum, W. E. H., 2017. Soil aggregation and soil organic matter in conventionally and organically farmed Austrian Chernozems. Die Bodenkultur: Journal of Land Management, Food and Environment 68 (1), 41–55.

Schäffer, B., Stauber, M., Müller, R., Schulin, R., 2007. Changes in the macro-pore structure of restored soil caused by compaction beneath heavy agricultural machinery: a morphometric study. Eur. J. Soil Sci. 58 (5), 1062–1073.

Schjønning, P., van den Akker, J. J. H., Keller, T., Greve, M. H., Lamandé, M., Simojoki, A., Stettler, M., Arvidsson, J., Breuning-Madsen, H., 2015. Driver-Pressure-State-Impact-Response (DPSIR) analysis and risk assessment for soil compaction - A European perspective. In: Sparks, D. L. (Ed.), Advances in Agronomy. Vol. 133 of Advances in Agronomy. Academic Press, Ch. 5, pp. 183–237.

Schjønning, P., McBride, R. A., Keller, T., Obour, P. B., 2017. Predicting soil particle density from clay and soil organic matter contents. Geoderma 286, 83–87.

Six, J., Elliott, E. T., Paustian, K., Doran, J. W., 1998. Aggregation and soil organic matter accumulation in cultivated and native grassland soils. Soil Sci. Soc. Am. J. 62 (5), 1367–1377.

Soil Survey Staff, 1999. A basic system of soil classification for making and interpreting soil surveys. Agricultural Handbook 436, Natural Resources Conservation Service, USDA, Washington DC, USA.

Stone, J. A., Larson, W. E., 1980. Rebound of five one-dimensionally compressed unsaturated granular soils. Soil Sci. Soc. Am. J. 44 (4), 819–822.

Styrelsen for Dataforsyning og Effektivisering, 2018. Grønland 1:250.000. https://download.kortforsyningen.dk/content/groenland-1250000, (Agency for Data Supply and Efficiency; visited online: March 24, 2021).

Terzaghi, K., 1925. Erdbaumechanik auf bodenphysikalischer Grundlage. F. Deuticke, Leipzig, Vienna.

Trükmann, K., Horn, R., Reintam, E., 2009. Impact of roots on soil stabilization in grassland. ISTRO 18th Triennial Conference Proceedings T4-022, 1–7.

Tukey, J. W., 1977. Exploratory Data Analysis. Addison-Wesley, Boston, Bonn.

Whalley, W. R., Dumitru, E., Dexter, A. R., 1995. Biological effects of soil compaction. Soil Tillage Res. 35 (1), 53–68.

Wiesmeier, M., Steffens, M., Mueller, C. W., Kölbl, A., Reszkowska, A., Peth, S., Horn, R., Kögel-Knabner, I., 2012. Aggregate stability and physical protection of soil organic carbon in semi-arid steppe soils. Eur. J. Soil Sci. 63 (1), 22–31.

IUSS Working Group WRB, 2015. World Reference Base for Soil Resources 2014, update 2015 International soil classification system for naming soils and creating legends for soil maps. World Soil Resources Reports No. 106. FAO, Rome.

Xie, S.-b., Jian-jun, Q., Yuan-ming, L., Zhi-wei, Z., Xiang-tian, X., 2015. Effects of freeze-thaw cycles on soil mechanical and physical properties in the Qinghai-Tibet plateau. J. Mt. Sci.-Engl. 12 (4), 999–1009.

Zhang, B., Horn, R., Hallett, P. D., May 2005. Mechanical resilience of degraded soil amended with organic matter. Soil Sci. Soc. Am. J. 69 (3), 864–871.

Zhang, H. Q., Hartge, K. H., 1990. Die Kohäsion ungesättigter Sandböden und deren Beeinflussung durch organische Substanz. Zeitschrift für Pflanzenernährung und Bodenkunde 3 (4), 311–326.

Zhang, X.-h., Li, L.-q., Pan, G.-x., 2007. Topsoil organic carbon mineralization and CO_2 evolution of three paddy soils from South China and the temperature dependence. J. Environ. Sci. 19 (3), 319–326.